JOTCSA
Journal of the Turkish Chemical Society
Section: A
Chemistry

TURKISH CHEMICAL SOCIETY

Preparation of Modified Surfaces Based on Tannic Acid and Carbon Nanotubes and Investigation of Their Electrochemical Properties

Hilal İncebay[1*], Rumeysa Saylakçı[1]

[1]Nevsehir Hacı Bektas Veli University, Department of Molecular Biology and Genetics, Nevsehir, 50300, Turkey.

Abstract: This study focuses on the electrochemical investigation of modifiers and their components that can provide the easiest and most sensitive results for electrochemical sensors. For this purpose, a nanocomposite of tannic acid and carbon nanotubes with extraordinary properties was obtained. The nanocomposite and its components were immobilized on glassy carbon electrode surfaces by the drop-drying technique. The morphological and electrochemical properties of the nanocomposite and its components were examined by scanning electron microscopy and cyclic voltammetry techniques. The surfaces modified with the nanocomposite and its components exhibited different electrochemical behaviors. Tests performed in ferricyanide, ferrocene, ruthenium hexamine (III) chloride, and ferricyanide/ferrocyanide probes showed that the nanocomposite-modified surface exhibited the best voltammetric behavior. Scan rate and pH studies showed that the nanocomposite-modified surface catalyzed electron transfer more and increased the active surface area.

Keywords: Carbon nanotube, Modification, Nanocomposite, Tannic acid.

Submitted: August 6, 2024. **Accepted:** September 27, 2024.

Cite this: İncebay H, Saylakçı R. Preparation of Modified Surfaces Based on Tannic Acid and Carbon Nanotubes and Investigation of Their Electrochemical Properties. JOTCSA. 2024;11(4): 1595-604.

DOI: https://doi.org/10.18596/jotcsa.1528731

***Corresponding author's E-mail:** hilalincebay@gmail.com

1. INTRODUCTION

Tannins are also known as tannic acid. Tannins are compounds with polyphenolic structures and are obtained from plants such as tea, rapeseed, broad bean, and sorghum. Tannic acid (TA) is present in numerous vegetables, fruits, and beverages, including wine, beer, coffee, black tea, and white tea. Simultaneously, due to the presence of numerous hydroxyl and functional groups in their structures, they are capable of forming cross-links with proteins and other macromolecules. TA, a water-soluble polyphenol compound, has been actively used to treat many diseases for years (1,2). TA analysis is gaining importance due to its wide range of studies, such as environment, medicine, and food. TA is used as a food additive and sweetener (3) as well as an additive in medicine and veterinary fields due to its antimicrobial, anticarcinogenic, and antimutagenic potential. At the same time, TA protects cells against oxidation properties (4,5). Determining the amount of tannic acid contained in fruit, tea, and beer is very important in evaluating the quality of the products (6). TA, which has a very wide area of use in medicine, is used in the treatment of tonsils, pharyngitis, hemorrhoids, and some diseases due to its astringent effects on vessels and mucosa. This compound also has antioxidant, antitumor, antimutagenic, and antiviral properties and other types of physiological activities (7-9). An important feature of TA is its strong interaction with metal ions, polymers, and proteins (10). The TA molecule contains a large number of active phenolic groups and is easily converted to polytannic acid (PTA), which can bind to various molecules through covalent or non-covalent bonds. Therefore, PTA has attracted great interest in surface modification due to its good adhesion, excellent biocompatibility, biodegradability, antimicrobial and antioxidant effects (11,12). In addition, thanks to its active phenolic groups, it easily forms composites by integrating with various molecules (13). Therefore, it can be effectively used as a modifier for electrochemical sensors.

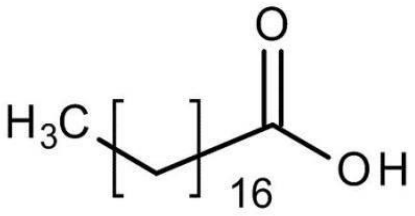

Scheme: The molecular formula of tannic acid.

Nowadays, it has been determined that nanocomposites are superior to pure polymers in terms of thermal, optical, mechanical, electronic, and catalytic properties. Studies have shown that the incorporation of nanoparticles in nanocomposites has several beneficial and enhancing effects (14). This is due to the fact that nanoparticles or nanostructured materials increase the adhesion/bonding between the matrix and nanostructured materials thanks to their large surface areas (15). In addition, the easy and homogeneous incorporation of nanostructures into the matrix also takes their positive effects to the next level. Considering these properties of nanostructures, carbon nanotubes (CNTs) are known to be the hardest and most durable man-made nanomaterials known so far (16). In addition to all the advantages they offer, they have also attracted interest in areas related to electrical devices and communication thanks to their high electrical conductivity properties (17,18). Moreover, due to their very small dimensions, these structures can also be used if they are homogeneously embedded in matrices. To increase the chemical affinity of carbon nanotubes (CNTs) to polymer matrices, chemical modification of graphitic sidewalls and ends is required. The properties and applications of CNTs have been very active areas of research in the last decade (19-23). CNTs exhibit high flexibility, low bulk density, and a large aspect ratio (typically greater than 1000). MWCNTs can transport electrons along long lengths without significant interruption, making them more conductive than copper (24). The main advantage of CNTs, which makes them ideal reinforcements for several applications, is that their mechanical and electrical properties can be utilized in combination (25,26).

TA is an oligomeric polymer of carbon-carbon bonded flavonoid units resistant to hydrolysis and can work in harmony with nanostructures during enzymatic/chemical reactions. This allows the integration of TA with carbon-based nanostructures or nanoparticles as a sensor interface to trigger the correct enzymatic reactions and significantly increase the detection capability of the modified electron. Thus, it provides the potential to provide innovative, fast, simple, durable, and accurate high-sensitivity measurements in the development of electrochemical sensor systems. The combination of carbon nanotubes with the advantageous features of tannic acid is anticipated to yield novel composite forms, offering cost-effective and efficient modifiers and facilitating the development of revolutionary electrochemical sensors (13).

This study aims to prepare a nanocomposite by taking advantage of the superior properties of tannic acidic active phenolic groups and multi-walled carbon nanotubes. For this purpose, the nanocomposite suspension prepared by sonication in chloroform was modified on glassy carbon electrode surfaces via the drop-drying technique. Tannic acid and multi-walled carbon nanotubes, which are the components constituting the nanocomposite, were also prepared in the same manner, and modified electrodes were obtained. Then, the electrochemical and morphological characteristics of the obtained surfaces were investigated and compared with both each other and the bare GCE.

2. EXPERIMENTAL SECTION

2.1. Materials

Potassium ferricyanide (≥99%), tannic acid (99%), ferrocene (98%), acetonitrile (%97), tetrabutylammonium tetrafluoroborate (99%), potassium ferrocyanide (99.9%), and chloroform (≥99.5%) were ensured by Merck, VWR, and Sigma-Aldrich. Carbon nanotubes (110–170 nm) were purchased from Sigma. Ultrapure water was used in aqueous solutions, acetonitrile was used in non-aqueous solutions, and all solutions were kept at +4°C. 99% pure $N_{2(g)}$ was used to remove dissolved oxygen in the cell before electrochemical experiments.

A Gamry Interface 1000B Potentiostat/Galvanostat/Zra analyzer was used for electrochemical experiments. In this analyzer, which has a three-electrode system, a nanocomposite-modified glassy carbon electrode (BASi Model MF–2012) served as the working electrode. The reference electrodes employed were the BASi model MF-2052 of Ag/AgCl/KCl (3M), the BASi model MF-2062 of Ag($AgNO_3$(0.1M)), and the counter electrode was a Pt wire (0.5mm).

2.2. Functionalization of MWCNTs

Before modification, commercial MWCNTs were sonicated in a concentrated $HClO_4$(98.5-102.0%) + HNO_3(96-98%) (3:7, v:v) solution for 5 h to functionalize their surfaces (27). The functionalized MWCNTs were then filtered, repeatedly washed with ultrapure water to neutralize, and dried at room temperature.

2.3. Preparation of Modifier Suspensions

MWCNTs suspension: prepared by sonicating 1 mg of MWCNTs within 5 mL chloroform for 1 h.

TA suspension: prepared by sonicating 1 mg of TA within 5 mL chloroform for 1 h. TA/MWCNTs suspension: prepared by sonicating 1 mg of MWCNTs within 5 mL chloroform for 5 min, then adding 10 mg TA to the solution and sonicating the solution for another 1 h.

2.4. Modification

After the preparation of MWCNTs, TA, and TA/MWCNTs suspensions, 5.0 µL of each suspension was immobilized on the cleaned glassy carbon electrode surfaces by the drop-drying technique. Three modified electrodes defined as MWCNTs/GCE, TA/GCE and TA/MWCNTs/GCE were obtained.

2.5. Characterization

For the morphological characterization, SEM images were taken of the MWCNTs/GCE, TA/GCE, and TA/MWCNTs/GCE surfaces at 1µm.

For the electrochemical characterization of bare GCE, TA/GCE, MWCNTs/GCE, and TA/MWCNTs/GCE surfaces with cyclic voltammetry (CV) technique in ferrocene, ferricyanide (HCF(III)), ruthenium hexaamine(III) chloride and ferri-ferrocyanide (HCF(III)-HCF(II)) redox probes, respectively;

- ✓ In 1.0 mM ferrocene solution, within the -0.2/+0.4 V range, at 100 mV/s scan rate, against $Ag/AgNO_3$ reference electrode,
- ✓ In 1.0 mM HCF(III) solution, within the +0.6/0.0 V range, at 100 mV/s scan rate, Ag/AgCl reference electrode, In 1.0 mM ruthenium hexamine(III) chloride solution, within the -0.5/0.2 V range, at 100 mV/s scan rate, against Ag/AgCl reference electrode,
- ✓ In 1.0 mM HCF(III)-(II) solution, within the -0.3/0.8 V range, at 100 mV/s scan rate, against Ag/AgCl reference electrode, voltammograms were recorded.

To provide insight into the TA, MWCNTs, and TA/MWCNTs structures to the GCE surface and to obtain information on whether there is an active group or groups that can be protonated on the surfaces after modification, voltammograms of each of the bare GCE, TA/GCE, MWCNTs/GCE and TA/MWCNTs/GCE surfaces were recorded separately on 1.0 mM HCF(III) probes prepared with BR buffer solutions at pH 2.0; 3.0; 5.0; 7.0; 9.0; and 11.0 (within the +0.6/0.0 V range, at 100 mV/s scan rate against an $Ag/AgCl/KCl_{(sat)}$ reference electrode).

To determine the electron transfer pattern of TA, MWCNTs and TA/MWCNTs structures on the GCE surface, voltammograms of each of the bare GCE, TA/GCE, MWCNTs/GCE, and TA/MWCNTs/GCE surfaces were recorded against the $Ag/AgNO_3$ reference electrode within the -0.2/0.4 V range in 1.0 mM ferrocene probe prepared in CH_3CN containing 100 mM TBA-TFB at scan rates of 25, 50, 100, 200, 300, 400, 500, 600, 700 mV/s.

3. RESULTS AND DISCUSSION

3.1. Scanning Electron Microscope Examination of MWCNTs/GCE, TA/GCE, and TA/MWCNTs GCE Surfaces

Elucidating the morphology of modified surfaces provides important ideas. For this reason, 1µm surface images of the prepared MWCNTs/GCE, TA/GCE, and TA/MWCNTs/GCE modified electrodes were recorded with the SEM technique and presented in Figure 1. When the SEM image of the MWCNTs/GCE surface given in Figure 1A is examined, it is observed that MWCNTs are homogeneously distributed on the GCE surface, and there is no agglomeration. In Figure 1B, it is observed that TA also exhibits a homogeneous distribution without agglomeration. When Figure 1C is examined, it is determined that the TA/MWCNTs/GCE surface exhibits a complex structure by homogeneously dispersing the structure of MWCNTs functionalized with the multi-armed polyphenol structure of TA and flavonoid oligomer polymers. The homogeneous dispersion of MWCNTs, one of the components forming the nanocomposite (TA/MWCNTs), into the TA structure, showed that the adhesion/bonding between the matrix and nanostructured materials increased thanks to the large surface areas of the nanostructured materials (15).

3.2. Electrochemical behaviors of Bare GCE, TA/GCE, MWCNTs/GCE, and TA/MWCNTs/GCE in Redox Probes

Electrochemical tests performed by cyclic voltammetry (CV) in the presence of redox probes are an effective method to reveal whether electron transfer occurs between the surface and the electrolyte. Therefore, the electrochemical behaviors of bare GCE, TA/GCE, MWCNTs/GCE, and TA/MWCNTs/GCE were individually examined using the CV technique in the presence of HCF(III), ferrocene, HCF(III) – HCF(II), and ruthenium hexamine(III) chloride probes. The electrochemical behaviors of the modified GCE surfaces were compared with the electrochemical behavior of the bare GCE surface. Figure 2A presents the voltammograms of bare GCE, MWCNTs/GCE, TA/GCE, and TA/MWCNTs/GCE in the HCF(III) probe within the 0.0/0.6 V range at 100 mV/s scan rate. The voltammograms reveal that the peak current for MWCNTs/GCE is higher than that for TA/GCE, which can be attributed to the large surface area of MWCNTs and their functional groups that enhance catalytic activity and conductivity on the electrode surface (28). TA/MWCNTs/GCE showed the best voltammetric response compared to TA/GCE and MWCNTs/GCE modified surfaces. This is due to the synergistic effect created by combining the functional groups within the structure of MWCNTs and groups in TA with a multi-armed polyphenolic structure (29,30). Therefore, we can say that this effect improves the sensing ability of the surface and increases the electrode surface area and conductivity, improving the electron transfer rate.

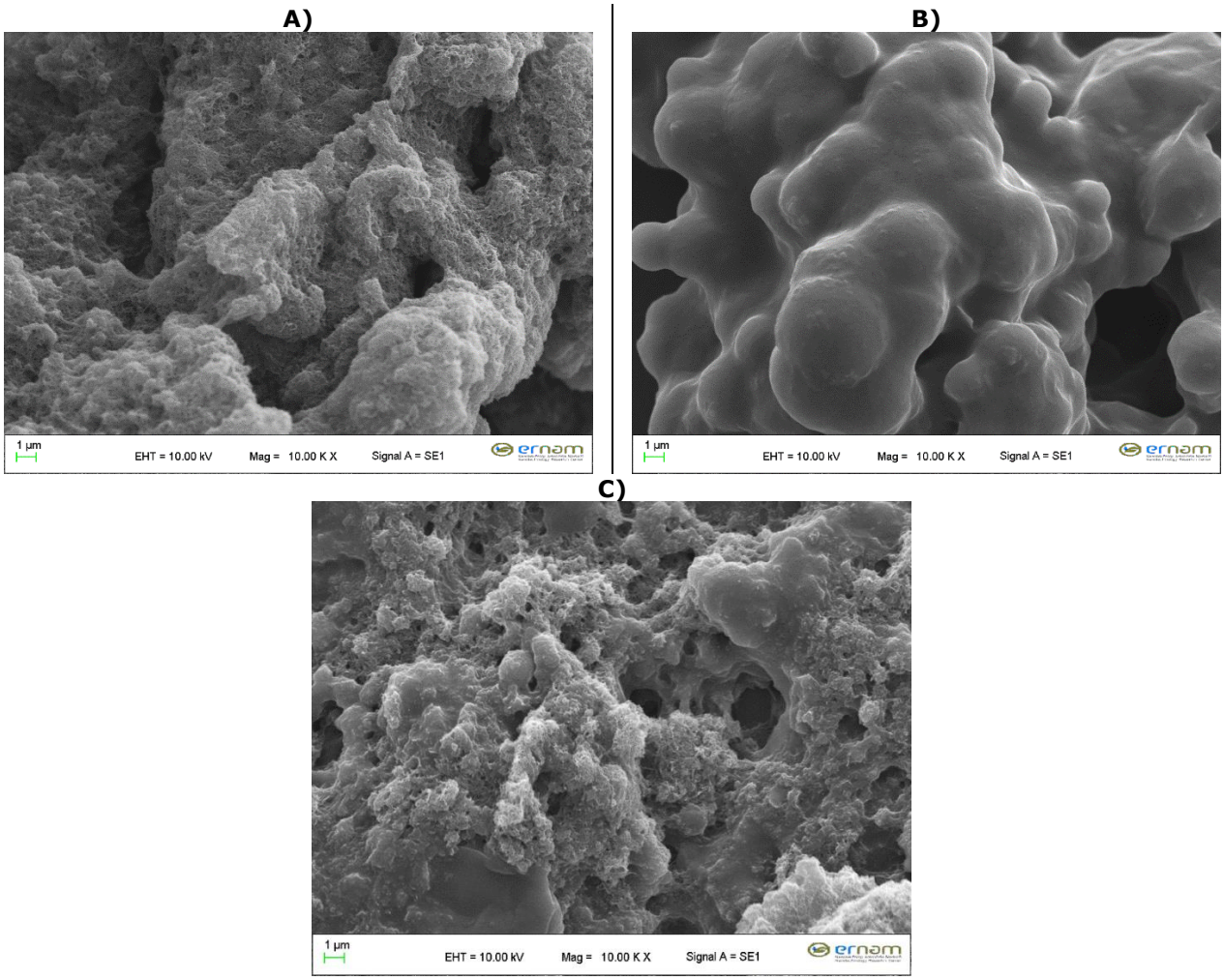

Figure 1: SEM micrograph **A)** MWCNTs/GCE, **B)** TA/GCE and **C)** TA/MWCNTs/GCE.

Figure 2B. represents the voltammograms of the ferrocene probe within the -0.2/0.4V range at 100 mV/s scan rate for the bare/GCE, TA/GCE, MWCNTs/GCE, TA/MWCNTs/GCE surfaces. The anodic peak currents of the bare GCE, TA/GCE, and MWCNTs/GCE surfaces are found to each other, while the TA/MWCNTs surface exhibits the highest peak current by showing the best electrocatalytic activity. This can be attributed to the formation of cross-links with electrochemical molecules with a large number of hydroxyl groups and functional groups in the structure of TA. In addition, due to the presence of a large number of active phenolic groups, it is also associated with the successful modification of the surface by transforming into a multiple TA structure that can adhere to various electrode surfaces through covalent or non-covalent bonds. Moreover, it has been observed that the composite structures used as modifier species do not make the electrode surface electro-inactive. Therefore, the voltammetric responses observed with the ferrocene probe indicated that electron transfer occurred on both the bare GCE and the modified GCE surfaces without any obstruction impeding the process (31,32).

Figure 2C shows the surface voltammograms for bare GCE, TA/GCE, MWCNTs/GCE, and TA/MWCNTs/GCE within the -0.3 to 0.8 V range at 100 mV/s scan rate using the HCF(III)-HCF(II) probe. Both reduction and oxidation peaks are visible on the bare GCE and modified GCE surfaces. This is due to the oxidation of Fe^{2+} ions to Fe^{3+} ions and the subsequent reduction of Fe^{3+} ions back to Fe^{2+} ions. Moreover, the voltammetric responses for the HCF(III)-HCF(II) probe show that while bare GCE and MWCNTs/GCE surfaces have similar peak currents and potential shifts, the TA/MWCNTs/GCE surface provides the most favorable voltammetric response. This improved performance is likely due to the excellent surface compatibility provided by the carbon-carbon bonded flavonoid units of TA, which are resistant to hydrolysis, in combination with functionalized carbon nanotubes on the surfaces (33). Thus, the electron transfer of TA/MWCNTs/GCE in the HCF(III)-HCF(II) probe was more catalyzed.

Figure 2D represents the voltammograms for bare GCE, TA/GCE, MWCNTs/GCE, and TA/MWCNTs/GCE surfaces within the -0.5 to 0.2 V range at 100 mV/s scan rate using the ruthenium hexaamine(III) chloride probe. All surfaces exhibit sensitivity to ruthenium for both reduction and oxidation reactions. While the bare GCE, MWCNTs/GCE, and TA/GCE surfaces show similar voltammetric responses to the ruthenium hexamine(III) chloride, the TA/MWCNTs/GCE surface demonstrates a more pronounced peak current. This enhanced sensitivity of the TA/MWCNTs/GCE surface to the ruthenium hexaamine(III) chloride probe may be attributed to TA's role as a compatible polymer material, forming

strong π-π interactions through the stacking of hydroxyl groups esterified with phenolic structures when combined with carbon-based nanostructures (34,35). It can be concluded that TA/MWCNTs/GCE significantly increases the detection capability and sensitivity thanks to this interaction.

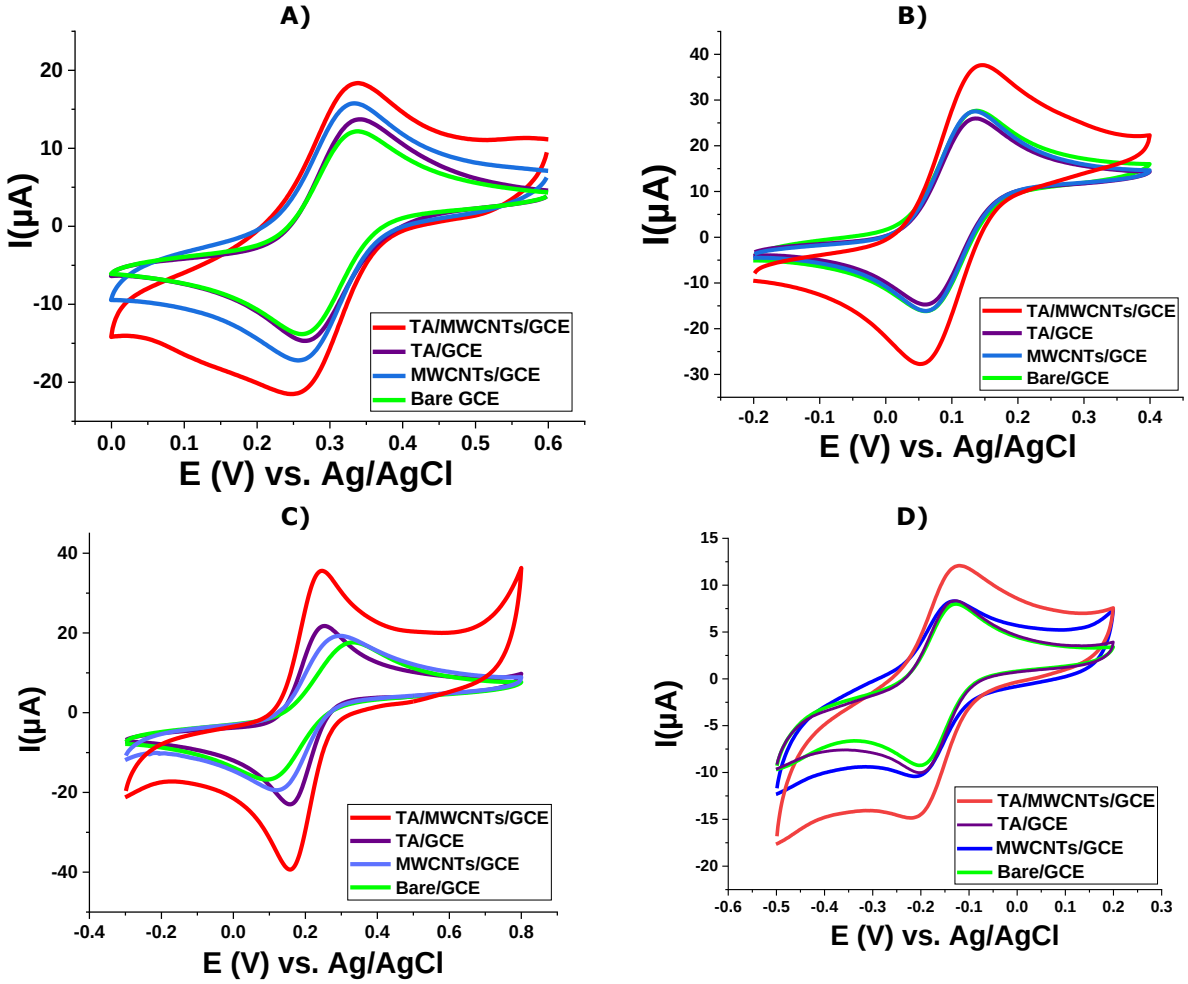

Figure 2: Surface voltammograms of bare/GCE, TA/GCE, MWCNTs/GCE, TA/MWCNT/GCE against at 100 mV/s scan rate **A)** Ag/AgCl/KCl(sat) reference electrode in 0.0/0.6 V potential range in 1.0 mM HCF(III); **B)** $Ag/AgNO_3$ reference electrode in the potential range of -0.2/0.4 V in 1.0 mM Ferrocene, **C)** Ag/AgCl/KCl(sat) reference electrode in the potential range of -0.3/0.8 V in 1.0 mM HCF(III)-HCF(II) solution **D)** against Ag/AgCl/KCl(sat) reference electrode in the potential range of -0.5/0.2 V in 1.0 mM ruthenium hexaamine(III) chloride solution.

5.3. pH Effect on Bare GCE, MWCNTs/GCE, TA/GCE and TA/MWCNTs/GCE Surfaces

The voltammetric responses of bare GCE, TA/GCE, MWCNTs/GCE and TA/MWCNTs/GCE surfaces in the +0.6–0.0 V potential range in the pH range from 2.0 to 11.0 in 1.0 Mm HCF(III) redox probe were investigated by CV technique and are presented in Figure 3. Peak currents were observed at pH 2.0 and 3.0 on bare GCE surface (Figure 3A). However, there were decreases in peak currents with increasing pH and peak currents were not observed at high pHs. Therefore, it was concluded that the bare GCE surface was sensitive to pH in acidic media. As presented in Figure 3B, the MWCNTs/GCE surface is sensitive to pH, but no peak current is observed on the surface at basic pH values such as pH 7.0, 9.0, 11.0, while a good peak current is obtained at acidic pH values, especially at pH 2.0. The reason for this decrease in peak currents with increasing pH can be associated with the negatively charged OH^- ions, which increase as a result of the basicity of the medium, repel the negatively charged HCF(III) ions, thus reducing electron transfer and thus decreasing the voltammetric peak currents of the MWCNTs/GGCE surface. In Figure 3C, it is observed that the TA/GCE surface gives similar peak currents with small shifts in peak potentials at pH 3.0, 5.0, 7.0 and 9.0, and the best voltammetric peak current occurs at pH 2.0. However, it is seen that it does not form a peak current by being blocked at basic pH values such as pH 11.0. It can be said that this situation is due to the repulsion of negatively charged molecules in TA and the OH^- ions that increase in the media at high pHs. It can also be explained by the fact that structures such as gallic acid and polyphenolic acid in the TA structure negatively affect the electron transfer on the surface and prevent the formation of a voltammetric response (36,37). As presented in Figure 3D, the TA/MWCNTs/GCE surface exhibits similar sensitivity at pH 3.0, 5.0, and 7.0. A well-defined peak current was obtained with a shift in the peak potential at pH 2.0. However, it was also determined that the surface was blocked at pH 11.0 and did not produce a peak current response. This

can be associated with the OH- groups attached to the carbohydrate (usually D-glucose) and phenolic groups in the center of the TA structure and the OH- ions abundant in the media at pH 11.0 repelling each other and negatively affecting the electrocatalytic activity of the modified surface. Experimental findings showed that the reactions of modified GCE surfaces in the HCF(III) redox probe were more reversible at low pH values.

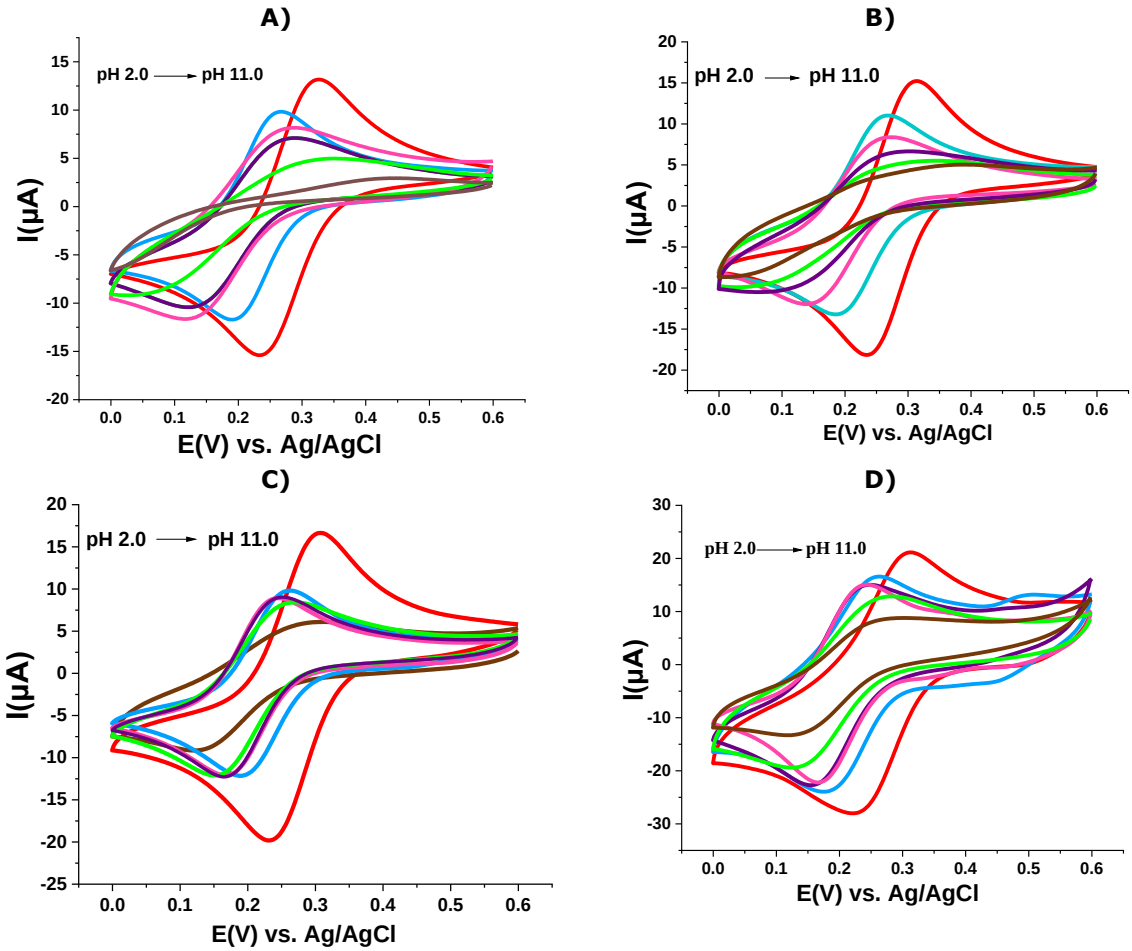

Figure 3: CV voltammograms of **A)** bare GCE, **B)** MWCNTs/GCE, **C)** TA/GCE, **D)** TA/MWCNTs/GCE surface in 1.0 mM HCF(III) probe against Ag/AgCl/$KCl_{(sat)}$ reference electrode in the potential range +0.6-0.0 V at 100 mV/s scan rate in the potential range +0.6-0.0 V at pH 2; 3; 5;7;9;11.

5.4. Scan Rate Effect on Bare GCE, TA/GCE, MWCNTs/GCE and TA/MWCNTs/GCE Surfaces

To investigate the properties such as reversibility and electron transfer pattern of bare GCE, TA/GCE, MWCNTs/GCE and TA/MWCNTs/GCE surfaces, voltammograms were recorded at 25, 50, 100, 200, 300, 400, 500, 600 and 700 mV/s scan rates against $Ag/AgNO_3$ reference electrode within the -0.2/0.4 V range using CV technique in 1.0 mM ferrocene probe and are presented in Figure 4A-D. While almost no change was observed in the peak potentials of all surfaces with the increasing scan rates, a linear increase in the peak currents was observed. The same situation occurred in the reverse scan. To better understand the reaction mechanism on the electrode surface, peak currents were plotted against both the scan rate and the square root of the scan rate. A linear relationship was observed between the peak currents and the square root of the scan rate (Figure 4E-H). For adsorption-controlled reactions on electrode surfaces, the graphs should be linear, and the slopes should be greater than 0.5. However, it is known that the reaction is diffusion-controlled if the slope value is less than 0.5 (38). The peak currents versus the square root of the scan rate were plotted, R^2 values were calculated, and it was found that R^2 = 0.9997 for the bare GCE surface, R^2 = 0.9977 for the MWCNTs surface, R^2 = 0.9989 for the TA/GCE surface, and R^2 = 0.9997 for the TA/MWCNTs/GCE surface. Since the obtained R^2 values were very close to 1.0 and the slope values were greater than 0.5, it was determined that the electrochemical reaction taking place on the bare GCE, MWCNTs/GCE, TA/GCE and TA/MWCNTs/GCE surfaces was an adsorption-controlled reaction.

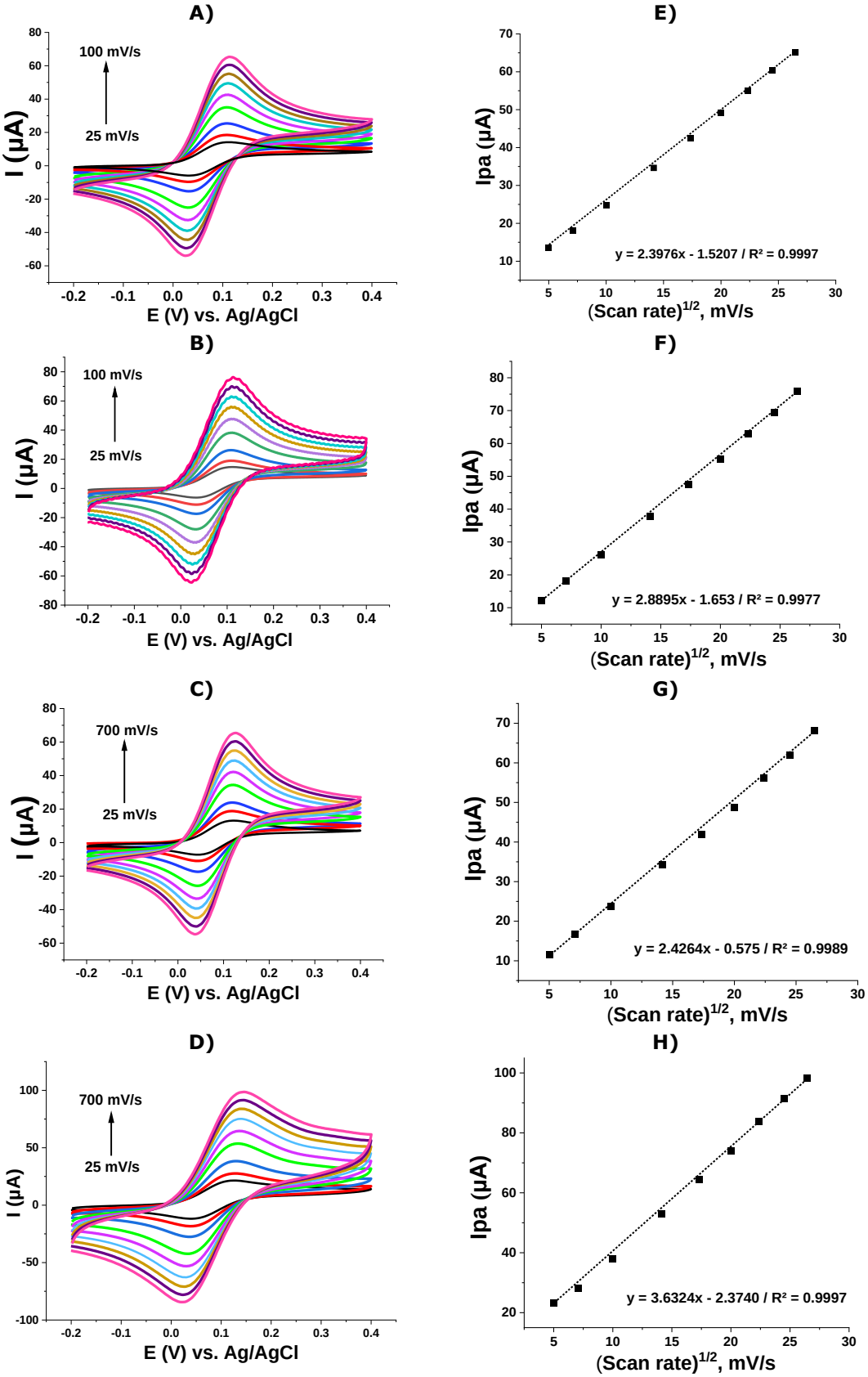

Figure 4: CV voltammograms of **A)** bare/GCE, **B)** MWCNTs/GCE, **C)** TA//GCE, **D)** TA/MWCNTs/GCE surface in 1.0 mM ferrocene solution against $Ag/AgNO_3$ reference electrode at scan rates of 25; 50; 100; 200; 300; 400; 500; 600; 700 mV/s. Peak currents plot against the square root of scan rate for **E)** bare/GCE, **F)** MWCNTs/GCE, **G)** TA//GCE, **H)** TA/MWCNTs/GCE.

4. CONCLUSION

This study focused on gaining features that are fast, easy, cheap, and environmentally friendly by using fewer chemicals for the preparation of nanocomposites, which are becoming increasingly popular. Superior properties were gained by incorporating carbon nanotubes into its structure using a natural polymer such as tannic acid. Homogeneous distribution of the components of the nanocomposite within each other was confirmed morphologically. As a result of detailed electrochemical examinations of the nanocomposite and its components, when the voltammograms of HCF(III), ruthenium hexamine (III) chloride, and HCF(III) – HCF(II) probes were compared, it was determined that the TA/MWCNTs/GCE surface exhibited the best voltammetric behavior. In pH studies, it was determined that the surfaces were sensitive to pH, and in scan rate studies, the electrochemical reaction taking place on the TA/MWCNTs/GCE surface was an adsorption-controlled reaction. The active surface areas were calculated as 0.124 cm^2 for GCE and 0.3405 cm^2 for TA/MWCNTs/GCE. This indicated that nanocomposite-modified electrode TA/MWCNTs/GCE has a large and active surface area and can be successfully used to detect analytes in electrochemical sensor technology (13).

5. CONFLICT OF INTEREST

The authors declare that they have no known competing financial interests or personal relationships that could have appeared to influence the work reported in this paper.

6. ACKNOWLEDGMENTS

We would like to thank Nevşehir Hacı Bektaş Veli University (NEÜ ABAP20F19) for their financial support.

7. REFERENCES

1. Orlowski P, Krzyzowska M, Zdanowski R, Winnicka A, Nowakowska J, Stankiewicz W, et al. Assessment of in vitro cellular responses of monocytes and keratinocytes to tannic acid modified silver nanoparticles. Toxicol Vitr [Internet]. 2013 Sep 1;27(6):1798–808. Available from: <URL>.

2. Ghasemian M, Kazeminava F, Naseri A, Mohebzadeh S, Abbaszadeh M, Kafil HS, et al. Recent progress in tannic acid based approaches as a natural polyphenolic biomaterial for cancer therapy: A review. Biomed Pharmacother [Internet]. 2023 Oct 1;166:115328. Available from: <URL>.

3. Ahmed GHG, Laíño RB, Calzón JAG, García MED. Fluorescent carbon nanodots for sensitive and selective detection of tannic acid in wines. Talanta [Internet]. 2015 Jan 15;132:252–7. Available from: <URL>.https://linkinghub.elsevier.com/retrieve/pii/S0039914014008030

4. Ren A, Zhang W, Thomas HG, Barish A, Berry S, Kiel JS, et al. A tannic acid-based medical food, cesinex®, exhibits broad-spectrum antidiarrheal properties: A mechanistic and clinical study. Dig Dis Sci [Internet]. 2012 Jan 12;57(1):99–108. Available from: <URL>.http://link.springer.com/10.1007/s10620-011-1821-9

5. Fu X, Yuan S, Yang F, Yu H, Xie Y, Guo Y, et al. Characterization of the interaction between boscalid and tannic acid and its effect on the antioxidant properties of tannic acid. J Food Sci [Internet]. 2023 Apr 14;88(4):1325–35. Available from: <URL>.

6. Anderson HE, Santos IC, Hildenbrand ZL, Schug KA. A review of the analytical methods used for beer ingredient and finished product analysis and quality control. Anal Chim Acta [Internet]. 2019 Nov 28;1085:1–20. Available from: <URL>.

7. Bigham A, Rahimkhoei V, Abasian P, Delfi M, Naderi J, Ghomi M, et al. Advances in tannic acid-incorporated biomaterials: Infection treatment, regenerative medicine, cancer therapy, and biosensing. Chem Eng J [Internet]. 2022 Mar 15;432:134146. Available from: <URL>.

8. Baldwin A, Booth BW. Biomedical applications of tannic acid. J Biomater Appl [Internet]. 2022 Mar 7;36(8):1503–23. Available from: <URL>.

9. Lee HY, Hwang CH, Kim HE, Jeong SH. Enhancement of bio-stability and mechanical properties of hyaluronic acid hydrogels by tannic acid treatment. Carbohydr Polym [Internet]. 2018 Apr 15;186:290–8. Available from: <URL>.

10. Higazy A, Hashem M, ElShafei A, Shaker N, Hady MA. Development of anti-microbial jute fabrics via *in situ* formation of cellulose–tannic acid–metal ion complex. Carbohydr Polym [Internet]. 2010 Mar 17;79(4):890–7. Available from: <URL>.

11. Oulad F, Zinadini S, Zinatizadeh AA, Derakhshan AA. Fabrication and characterization of a novel tannic acid coated boehmite/PES high performance antifouling NF membrane and application for licorice dye removal. Chem Eng J [Internet]. 2020 Oct 1;397:125105. Available from: <URL>.

12. Sahiner N, Sagbas S, Aktas N, Silan C. Inherently antioxidant and antimicrobial tannic acid release from poly(tannic acid) nanoparticles with controllable degradability. Colloids Surfaces B Biointerfaces [Internet]. 2016 Jun 1;142:334–43. Available from: <URL>.

13. Saylakcı R, Incebay H. An electrochemical platform of tannic acid and carbon nanotubes for the sensitive determination of the antipsychotic medication clozapine in pharmaceutical and biological samples. J Electroanal Chem [Internet]. 2021 Oct 1;898:115638. Available from: <URL>.

14. Çiçek Ozkan B, Güner M, Şeker TS. Thermal and morphological properties of HDPE/ZnO and HDPE/HAp nanocomposites. Fırat Univ J Eng Sci [Internet]. 2020 Mar 3;32(1):259–66. Available from: <URL>.

15. Langat J, Bellayer S, Hudrlik P, Hudrlik A, Maupin PH, Gilman JW, et al. Synthesis of imidazolium salts and their application in epoxy montmorillonite nanocomposites. Polymer (Guildf) [Internet]. 2006 Sep 7;47(19):6698–709. Available from: <URL>.

16. Ali A, Rahimian Koloor SS, Alshehri AH, Arockiarajan A. Carbon nanotube characteristics and enhancement effects on the mechanical features of polymer-based materials and structures – A review. J Mater Res Technol [Internet]. 2023 May 1;24:6495–521. Available from: <URL>.

17. Ben Messaoud N, Ghica ME, Dridi C, Ben Ali M, Brett CMA. Electrochemical sensor based on multiwalled carbon nanotube and gold nanoparticle modified electrode for the sensitive detection of bisphenol A. Sensors Actuators B Chem [Internet]. 2017 Dec 1;253:513–22. Available from: <URL>.

18. Mehmandoust M, Khoshnavaz Y, Tuzen M, Erk N. Voltammetric sensor based on bimetallic nanocomposite for determination of favipiravir as an antiviral drug. Microchim Acta [Internet]. 2021 Dec 27;188(12):434. Available from: <URL>.

19. Incebay H, Aktepe L, Leblebici Z. An electrochemical sensor based on green tea extract for detection of Cd(II) ions by differential pulse anodic stripping voltammetry. Surfaces and Interfaces [Internet]. 2020 Dec 1;21:100726. Available from: <URL>.

20. Valenzuela-Muñiz AM, Alonso-Nuñez G, Miki-Yoshida M, Botte GG, Verde-Gómez Y. High electroactivity performance in Pt/MWCNT and PtNi/MWCNT electrocatalysts. Int J Hydrogen Energy [Internet]. 2013 Sep 19;38(28):12640–7. Available from: <URL>.

21. Power AC, Gorey B, Chandra S, Chapman J. Carbon nanomaterials and their application to electrochemical sensors: A review. Nanotechnol Rev [Internet]. 2018 Feb 23;7(1):19–41. Available from: <URL>.

22. Shahrokhian S, Rastgar S, Amini MK, Adeli M. Fabrication of a modified electrode based on Fe_3O_4NPs/MWCNT nanocomposite: Application to simultaneous determination of guanine and adenine in DNA. Bioelectrochemistry [Internet]. 2012 Aug 1;86:78–86. Available from: <URL>.

23. Tigari G, Manjunatha JG. A surfactant enhanced novel pencil graphite and carbon nanotube composite paste material as an effective electrochemical sensor for determination of riboflavin. J Sci Adv Mater Devices [Internet]. 2020 Mar 1;5(1):56–64. Available from: <URL>.

24. Ali Z, Yaqoob S, Yu J, D'Amore A. Critical review on the characterization, preparation, and enhanced mechanical, thermal, and electrical properties of carbon nanotubes and their hybrid filler polymer composites for various applications. Compos Part C Open Access [Internet]. 2024 Mar 1;13:100434. Available from: <URL>.

25. Guldi DM, Rahman GMA, Zerbetto F, Prato M. Carbon nanotubes in electron donor–acceptor nanocomposites. Acc Chem Res [Internet]. 2005 Nov 1;38(11):871–8. Available from: <URL>.

26. Rathinavel S, Priyadharshini K, Panda D. A review on carbon nanotube: An overview of synthesis, properties, functionalization, characterization, and the application. Mater Sci Eng B [Internet]. 2021 Jun 1;268:115095. Available from: <URL>.

27. Kutluay A, Aslanoglu M. An electrochemical sensor prepared by sonochemical one-pot synthesis of multi-walled carbon nanotube-supported cobalt nanoparticles for the simultaneous determination of paracetamol and dopamine. Anal Chim Acta [Internet]. 2014 Aug 11;839:59–66. Available from: <URL>.

28. Niu JJ, Wang JN, Jiang Y, Su LF, Ma J. An approach to carbon nanotubes with high surface area and large pore volume. Microporous Mesoporous Mater [Internet]. 2007 Mar 23;100(1–3):1–5. Available from: <URL>.

29. Salinas-Torres D, Huerta F, Montilla F, Morallón E. Study on electroactive and electrocatalytic surfaces of single walled carbon nanotube-modified electrodes. Electrochim Acta [Internet]. 2011 Feb 1;56(5):2464–70. Available from: <URL>.

30. Moore KE, Flavel BS, Yu J, Abell AD, Shapter JG. Increased redox-active peptide loading on carbon nanotube electrodes. Electrochim Acta [Internet]. 2013 Feb 1;89:206–11. Available from: <URL>.

31. Fagan-Murphy A, Kataria S, Patel BA. Electrochemical performance of multi-walled carbon nanotube composite electrodes is enhanced with larger diameters and reduced specific surface area. J Solid State Electrochem [Internet]. 2016 Mar 6;20(3):785–92. Available from: <URL>.

32. Guan JF, Zou J, Liu YP, Jiang XY, Yu JG. Hybrid carbon nanotubes modified glassy carbon electrode for selective, sensitive and simultaneous detection of dopamine and uric acid. Ecotoxicol Environ Saf [Internet]. 2020 Sep 15;201:110872. Available from: <URL>.

33. Krywko-Cendrowska A, Marot L, Mathys D, Boulmedais F. Ion-imprinted nanofilms based on tannic acid and silver nanoparticles for sensing of Al(III). ACS Appl Nano Mater [Internet]. 2021 May 28;4(5):5372–82. Available from: <URL>.

34. Liao W, Yu C, Peng Z, Xu F, Zhang Y, Zhong W. Ultrasensitive Mg^{2+}-modulated carbon nanotube/tannic acid aerogels for high-performance wearable pressure sensors. ACS Sustain Chem Eng [Internet]. 2023 Feb 13;11(6):2186–97. Available from: <URL>.

35. Kruusenberg I, Alexeyeva N, Tammeveski K. The pH-dependence of oxygen reduction on multi-walled carbon nanotube modified glassy carbon electrodes. Carbon N Y [Internet]. 2009 Mar 1;47(3):651–8. Available from: <URL>.

36. Rai P, Mehrotra S, Sharma SK. Development of a

paper-based chromogenic strip and electrochemical sensor for the detection of tannic acid in beverages. LWT [Internet]. 2022 Nov 1;169:113999. Available from: <URL>.

37. Xu L, He N, Du J, Deng Y, Li Z, Wang T. A detailed investigation for determination of tannic acid by anodic stripping voltammetry using porous electrochemical sensor. Anal Chim Acta [Internet]. 2009 Feb 16;634(1):49–53. Available from: <URL>.

38. Lin CS, Denton EB, Gaskill HS, Putnam GL. Diffusion-controlled electrode reactions. Ind Eng Chem [Internet]. 1951 Sep 1;43(9):2136–43. Available from: <URL>.